

## Biocatalysis

Hydrolysis of Hydrophobic Esters in a Bicontinuous Microemulsion Catalysed by Lipase B from *Candida antarctica*Anne K. Steudle,<sup>[b]</sup> Mireia Subinya,<sup>[a]</sup> Bettina M. Nestl,<sup>[c]</sup> and Cosima Stubenrauch<sup>\*,[a]</sup>

**Abstract:** Selective enzyme-catalysed biotransformations offer great potential in organic chemistry. However, special requirements are needed to achieve optimum enzyme activity and stability. A bicontinuous microemulsion is proposed as reaction medium because of its large connected interface between oil and water domains at which a lipase can adsorb and convert substrates in the oil phase of the microemulsion. Herein, a microemulsion consisting of buffer-*n*-octane-nonionic surfactant C<sub>8</sub>E<sub>3</sub> was used to investigate the key factors that determine hydrolyses of *p*-nitrophenyl esters catalysed by the lipase B from *Candida antarctica* (CalB). The

highest CalB activity was found around 44 °C in the absence of NaCl and substrates with larger alkyl chains were better hydrolysed than their short-chained homologues. The CalB activity was determined using two different co-surfactants, namely the phospholipid 1,2-dioleoyl-*sn*-glycero-3-phosphocholine (DOPC) and the sugar surfactant decyl β-D-glucopyranoside (β-C<sub>10</sub>G<sub>1</sub>). The results show the CalB activity as linear function of both enzyme and substrate concentration with an enhanced activity when the sugar surfactant is used as co-surfactant.

## Introduction

Lipases (EC 3.1.1.3) hydrolyse in vivo triglycerides at an oil/water interface and belong to the class of hydrolases.<sup>[1]</sup> Most lipases possess a lid that covers the active site in an aqueous environment and opens in contact with a hydrophobic phase,<sup>[2]</sup> so-called interfacial activation. Since bicontinuous microemulsions have a very large oil/water interface,<sup>[3]</sup> we investigated them as the reaction media for hydrolytic reactions catalysed by lipases. The general composition of the microemulsion was buffer-*n*-octane-surfactant. Lipase B from *Candida antarctica* (CalB) was chosen because of its high stereoselectivity,<sup>[4]</sup> its well-known crystal structure, reaction mechanism and conformational stability in both hydrophilic and hydrophobic environments.<sup>[5]</sup> In contrast to other lipases, CalB does not undergo conformational changes by being adsorbed at an interface. This can be attributed to the fact that CalB does not possess a lid at the entrance of the active site.

Due to the fact that biocatalysts provide high substrate specificity, good yields, almost no side-products, less purification

steps and reduced waste output, biotechnological processes are often preferred to purely chemical approaches.<sup>[6]</sup> Lipases are known to be versatile biocatalysts and numerous reviews can be found describing the properties and applications of lipases in industry and research.<sup>[1,7]</sup> However, some biotechnological processes still lack competitive space-time yields, sustainable reaction conditions or high enantiopurities.

In this work we focus on lipase-catalysed hydrolysis reactions. Applications of this type of reaction are the kinetic resolution of racemic mixtures to generate small, optically pure molecules like chiral alcohols and amines<sup>[8]</sup> and the direct asymmetric synthesis of drugs, for example profens, which are among the most important non-steroidal anti-inflammatory drugs.<sup>[9]</sup> A challenge is often the limited solubility of non-polar substrates, even in mixed aqueous-organic systems. We intend to overcome these solubility limits by using bicontinuous microemulsions as reaction medium in which the aqueous phase hosts the enzyme, whereas the substrate is dissolved in the oil phase. Contact between enzyme and substrate is facilitated through the interfacial layer.

Lipase activity has been studied intensely in water/oil (w/o)-microemulsions<sup>[10,11]</sup> but only few studies have yet been reported on enzyme-catalysed reactions in bicontinuous microemulsions.<sup>[12]</sup> We chose to use the latter one because, in contrast to droplet microemulsions, bicontinuous microemulsions provide a connected interface between water and oil. In this paper, we want to identify key parameters for lipase-catalysed hydrolysis reactions in bicontinuous microemulsions. For this purpose, microemulsions prepared with alkyl polyglycol ethers C<sub>8</sub>E<sub>3</sub> as amphiphilic compound were chosen to take advantage of a wide range of accessible homologues without changing the overall nature of the surfactant.

[a] Dr. M. Subinya, Prof. Dr. C. Stubenrauch  
Institute of Physical Chemistry, University of Stuttgart  
Pfaffenwaldring 55, 70569 Stuttgart (Germany)  
E-mail: cosima.stubenrauch@ipc.uni-stuttgart.de

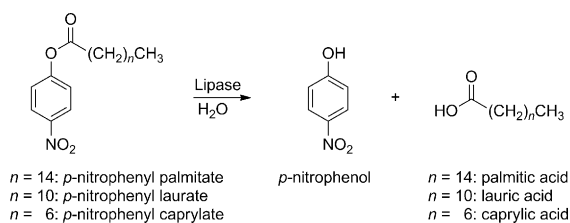
[b] A. K. Steudle  
Chemistry Department, Durham University  
South Road, DH1 3LE Durham (UK)

[c] Dr. B. M. Nestl  
Institute of Technical Biochemistry, University of Stuttgart  
Allmandring 31, 70569 Stuttgart (Germany)

Supporting information for this article is available on the WWW under <http://dx.doi.org/10.1002/chem.201405335>.

For this endeavour we address four key points: 1) The determination of the phase behaviour and the partitioning of the substrate in the microemulsion, 2) the effect of temperature and NaCl content on the CalB activity, 3) the investigation of the reaction kinetics by using different enzyme and substrate concentrations and 4) the effect of co-surfactants on the CalB activity. The hydrophilic sugar surfactant *n*-decyl- $\beta$ -D-glucopyranoside ( $\beta$ -C<sub>10</sub>G<sub>1</sub>) and the hydrophobic phospholipid 1,2-dioleoyl-*sn*-glycero-3-phosphocholine (DOPC) were used as co-surfactants.

The well-described hydrolysis of *p*-nitrophenyl esters to *p*-nitrophenol and fatty acid was chosen as the model reaction (Scheme 1) because this reaction is typically used to determine lipase activities in both aqueous reaction media<sup>[13,14]</sup> and w/o-microemulsions.<sup>[15]</sup> This reaction allows the photometric determination of the reaction rate by monitoring the *p*-nitrophenol concentration as a function of time at the isosbestic wavelength.



**Scheme 1.** Lipase-catalysed hydrolysis of the *p*-nitrophenyl esters with different chain lengths to *p*-nitrophenol and the respective fatty acid.

## Results

### Phase behaviour of microemulsions

The phase behaviour of microemulsions prepared with equal volumes of oil and water ( $\phi=0.5$ ) can be measured as a function of the temperature  $T$  and the surfactant mass fraction  $\gamma$ . At the phase inversion temperature  $\tilde{T}$ , a three-phase region is formed at low surfactant mass fractions  $\gamma < \tilde{\gamma}$ , and a single phase microemulsion at higher surfactant mass fractions  $\gamma > \tilde{\gamma}$ . Defined by  $\tilde{\gamma}$  and  $\tilde{T}$ , the  $X$ -point can be used to describe and compare the phase behaviour of different microemulsions. It is to be noted that a substrate or an enzyme added to a microemulsion might change the phase behaviour. The same holds true for products generated during the reaction. Accordingly, it is extremely important to study the influence of substrate, product and enzyme on the phase behaviour prior to the reaction. This allows counteracting and thus preventing any changes of the phase behaviour, that is, of the microstructure, during the reaction. The influence of CalB on the phase behaviour of the microemulsion system H<sub>2</sub>O/NaCl (CalB)-*n*-octane-C<sub>10</sub>E<sub>5</sub> was published previously and showed that an increase of CalB concentration in the microemulsion system shifts the phase inversion temperature  $\tilde{T}$  to lower values and that  $\tilde{\gamma}$  passes a minimum with increasing CalB concentration.<sup>[16]</sup> The phase behaviour of the CalB-containing microemulsions combined with the partitioning studies revealed that 80–90% of

the CalB molecules are located at the interfacial layer, whereas the rest is located in the water domain of the microemulsion.<sup>[16]</sup> In the following, the influence of one substrate and two products on the phase behaviour of microemulsions containing buffer/4 wt% NaCl/*p*-nitrophenol-*n*-octane/*p*-nitrophenyl palmitate/palmitic acid-C<sub>10</sub>E<sub>5</sub> is presented. Note that throughout this work, 100 mM TRIS pH 7 (buffer) is used as an aqueous phase to prepare the microemulsion. By way of an example, the influence of *p*-nitrophenyl palmitate, *p*-nitrophenol and palmitic acid is shown in Figure 1. All additives were dissolved in the aqueous or oil phase of the microemulsion at a concentration of 20 mM. The oil-soluble additives *p*-nitrophenyl palmitate and palmitic acid were found to shift the  $X$ -point of the microemulsion to lower phase inversion temperatures  $\tilde{T}$  and lower surfactant mass fractions  $\tilde{\gamma}$ . This effect of polar additives on the phase behaviour is well known and hence expected.<sup>[17]</sup> The water-soluble additive *p*-nitrophenol showed no effect on the efficiency of the microemulsions (i.e., on  $\tilde{\gamma}$ ), however the phase inversion temperature  $\tilde{T}$  decreased. To avoid changes in the composition of the microemulsion during the reaction, the surfactant mass fraction and temperature at which the reaction was carried out were chosen such that the one-phase region is not left during the reaction. In other words, by choosing a surfactant mass fraction that was high enough to overlap the one-phase regions of substrate-containing and CalB-containing microemulsions, changes of the phase behaviour during the reaction could be prevented. Additionally, we determined the reaction rates from the first 20 min of the reaction to minimise the influence of the products on the phase behaviour. Whether the one-phase region was indeed not left was checked visually after each measurement.

### Partitioning of substrates

To gain a deeper understanding of the reaction kinetics of the CalB-catalysed hydrolysis, the location of the substrate in the microemulsion was investigated. The aim is to facilitate the hydrolysis of a hydrophobic carboxylate ester, which is located in the oil domain of the microemulsion and is converted by the CalB at the interfacial layer. To prove that *p*-nitrophenyl palmitate is only located in the oil domain of the microemulsion, samples were prepared in the three-phase region. The advantage of a three-phase system is the fact that the compositions of oil and water excess phases can be approximated to be the same as the respective domains in the middle-phase microemulsion possessing a bicontinuous microstructure.

Therefore, a three-phase system was prepared and each of the phases analysed by UV/Vis spectroscopy. The three-phase system consisted of buffer/4 wt% NaCl-*n*-octane/5 mM *p*-nitrophenyl palmitate-C<sub>10</sub>E<sub>5</sub> (phase diagram in Figure 1) with a surfactant mass fraction of  $\gamma = 0.08$ . Figure 2 shows the spectra of *p*-nitrophenyl palmitate in the oil excess phase, the microemulsion middle phase and the water excess phase. The oil excess phase shows the highest absorbance, according to which the *p*-nitrophenyl palmitate is mainly dissolved in the oil domain. The water excess phase did not show any absorbance indicat-

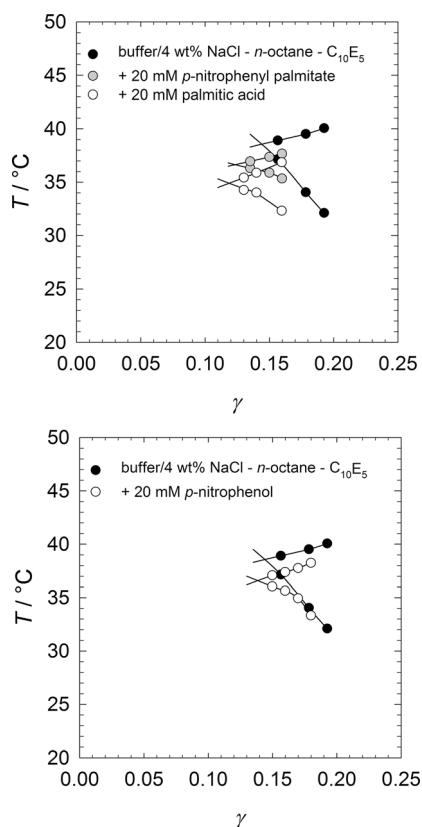


**Figure 1.** Phase diagrams of microemulsions consisting of buffer pH 7/4 wt% NaCl-*n*-octane- $C_{10}E_5$  as a function of  $T$  and  $\gamma$ . Influence of the oil-soluble additives *p*-nitrophenyl palmitate and palmitic acid (top) as well as of the water-soluble additive *p*-nitrophenol (bottom). The oil-to-water ratio was kept constant at  $\phi=0.5$ .

ing no *p*-nitrophenyl palmitate in the water domain of the microemulsion. The microemulsion phase showed about half the absorbance of the oil excess phase due to the volume fraction of oil being  $\phi=0.5$ . Additionally, the wavelength of maximum absorbance remained at 267 nm for all spectra, which is the same as observed in a stock solution of *p*-nitrophenyl palmitate prepared in *n*-octane. This indicates that the polarity of the environment did not change. These results demonstrate that *p*-nitrophenyl palmitate is only located in the oil domain of the microemulsion, and neither dissolved in the water phase nor adsorbed at the interfacial layer. The same result was obtained for substrates with different lengths of alkyl chains, namely *p*-nitrophenyl laurate and caprylate, as can be seen in Figure S1 in the Supporting Information.

### Effect of the NaCl content and temperature on the CalB activity

Temperature and ionic strength are known to influence enzymatic activities. Kinetic measurements over a range of temperatures or at different salt contents can clarify the optimal reaction conditions of the enzyme. To independently study the effect of temperature and NaCl content  $\varepsilon$  on the CalB activity in bicontinuous microemulsions, the hydrophilicity of the surfactant was changed such that different phase inversion tem-

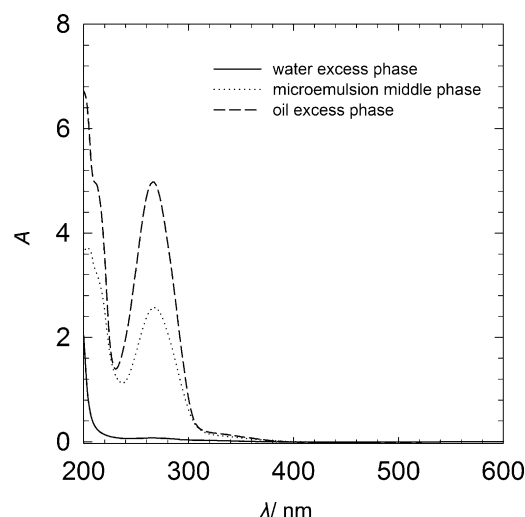


**Figure 2.** UV/Vis spectra of the individual phases of three-phase system. The microemulsions were prepared at  $\gamma=0.08$  and  $\phi=0.5$ . The sample consisted of buffer pH 7/4 wt% NaCl-*n*-octane/5 mM *p*-nitrophenyl palmitate- $C_{10}E_5$ .

peratures at constant  $\varepsilon$  as well as similar phase inversion temperatures at different  $\varepsilon$  are accessible.

We examined first the influence of the NaCl content  $\varepsilon$  on the CalB activity. For NaCl, contents of  $\varepsilon=0, 0.04, 0.11$  and  $0.18$  in the aqueous phase of the microemulsion the hydrophilicity of the surfactant was increased stepwise to obtain phase inversion temperatures around  $36^\circ\text{C}$  (Table 1). Phase diagrams of microemulsions consisting of buffer/NaCl-*n*-octane/5 mM *p*-nitrophenyl palmitate- $C_{10}E_j$  were measured and the CalB activity in the respective microemulsion was determined.

**Table 1.** X-points of the systems consisting of buffer pH 7/NaCl-*n*-octane/5 mM *p*-nitrophenyl palmitate- $C_{10}E_j$ .<sup>[a]</sup>

$j$	$\varepsilon$	$\tilde{\gamma}$	$\gamma_{\text{Reaction}}$	$\tilde{T}$ [ $^\circ\text{C}$ ]	$k_2$ [ $10^{-3} \text{ L s}^{-1} \text{ g}^{-1}$ ]
4.5	0	0.121	0.141	34	$0.0817 \pm 0.0064$
5	0.04	0.128	0.148	36	$0.0610 \pm 0.0014$
6	0.11	0.156	0.176	37	$0.0074 \pm 0.0004$
7	0.18	0.159	0.179	35	$0.0033 \pm 0.0002$

[a] For each system, the salt content  $\varepsilon$  and the number of ethylene glycol groups  $j$  is indicated. The CalB activity in each system is given by the observed second order rate constant  $k_2$ .

The  $\gamma$  used for the reactions was  $\gamma_{\text{Reaction}} = \tilde{\gamma} + 0.02$ . The CalB activities are given as observed second order rate constants  $k_2$ , which were calculated from the initial reaction rate divided by the enzyme and substrate concentration. The results are summarized in Table 1, in which the X-point of the phase diagrams are given for each NaCl content along with the observed second order rate constants  $k_2$ . As one can see, the observed second order rate constant  $k_2$  decreases significantly with increasing NaCl concentrations and thus the addition of NaCl was avoided wherever possible. With respect to the influence of the temperature (measurements were carried out between

34 and 37 °C, see Table 1) it was shown that the CalB activity slightly increases with temperature until it starts to unfold and loose activity at about 45–55 °C.<sup>[13,18]</sup> However, in the study at hand, the highest CalB activity was measured at the lowest temperature. Thus temperature cannot be the dominating parameter in our case. One also sees that the  $\tilde{\gamma}$ -values and thus the  $\gamma_{\text{Reaction}}$ -values shift towards slightly higher values with increasing NaCl concentration. To test whether changes of the surfactant mass fraction  $\gamma$  influence the CalB activity, we performed reactions in a range from  $\gamma_{\text{Reaction}} = \tilde{\gamma} + 0.01$  to  $\gamma_{\text{Reaction}} = \tilde{\gamma} + 0.05$ . Since we found no differences in the activity, we can readily say that the  $k_2$  values reflect the dependence on the NaCl concentration.

To study the effect of temperature on the CalB activity, all microemulsions were prepared without NaCl ( $\varepsilon = 0$ ). The studied systems consisted of buffer-*n*-octane/5 mm *p*-nitrophenyl palmitate- $\text{C}_{10}\text{E}_j$  with  $j = 4, 4.5, 5$  and  $5.5$  ( $j = 4.5$  means a 1:1 mixture of  $\text{C}_{10}\text{E}_4$  and  $\text{C}_{10}\text{E}_5$ ). The respective phase diagrams are presented in Figure 3 (top), in which the surfactant mass fractions used for the reaction  $\gamma_{\text{Reaction}}$  are also indicated. As can be seen in Figure 3 (top) the phase diagrams are shifted such that measurements at  $T = 23, 34, 44$  and  $51$  °C could be carried out. As mentioned above, slight changes in  $\tilde{\gamma}$  do not influence the activity. Figure 3 (bottom) illustrates the observed second order rate constants  $k_2$  for each temperature. The CalB activity shows a bell-shaped dependence on the temperature, which is well known from enzyme-catalysed reactions. This shape is explained by the increase of the reaction rate with temperature as described by Arrhenius, which is counteracted by the thermal deactivation of the enzyme at higher temperatures. The highest CalB activity was obtained in the microemulsion prepared with buffer-*n*-octane/5 mm *p*-nitrophenyl palmitate- $\text{C}_{10}\text{E}_5$  at  $T = 44$  °C and  $\gamma_{\text{Reaction}} = 0.175$ . Consequently, we have chosen this system to be our model system for the following studies wherever possible and feasible.

### Influence of the chain length of the substrate and the concentration on the CalB activity

To elucidate the impact of the length of the alkyl chain and concentration of the substrate on the CalB activity, the hydrolysis of substrates with different chain lengths were investigated. Moreover, the concentration was increased for one of them. Three substrates were tested, namely *p*-nitrophenyl palmitate, *p*-nitrophenyl laurate and *p*-nitrophenyl caprylate. To study CalB activity with increasing substrate concentrations, *p*-nitrophenyl laurate was used. In conventional aqueous reaction media, these substrates cannot be solubilised without the addition of detergents, and especially the *p*-nitrophenyl palmitate shows severe solubility problems. The reactions were carried out in microemulsions at 44 °C consisting of buffer-*n*-octane/substrate- $\text{C}_{10}\text{E}_5$  ( $\gamma_{\text{Reaction}} = 0.175$ ), which we have identified to be the most promising system regarding the activity of CalB. Phase diagrams containing 5 mm of the different substrates did not exhibit any differences (see also Figure S2 in the Supporting Information). Figure 4 shows the amount of *p*-

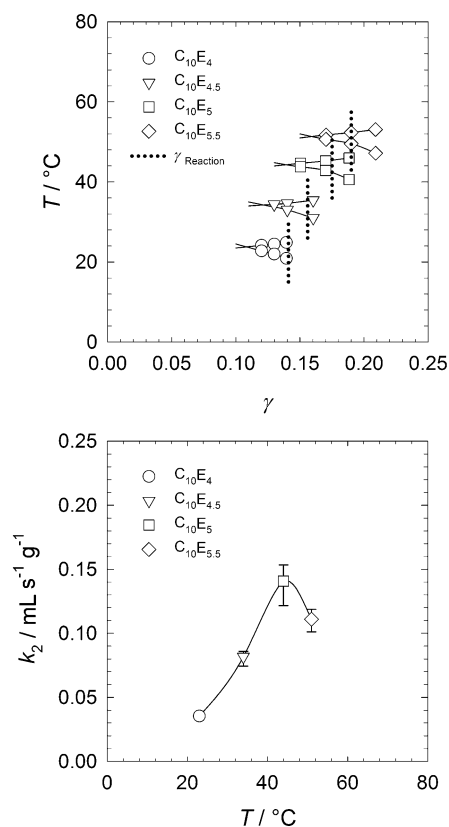


**Figure 3.** Top: phase diagrams of microemulsions consisting of buffer pH 7-*n*-octane (5 mm *p*-nitrophenyl palmitate)- $\text{C}_{10}\text{E}_j$  with  $j = 4; 4.5; 5; 5.5$ . The oil-to-water ratio was kept constant at  $\phi = 0.5$ . The phase inversion temperature  $\tilde{T}$  and the surfactant mass fraction  $\gamma_{\text{Reaction}} = \tilde{\gamma} + 0.02$  were used for the kinetic measurements. Bottom: influence of the temperature on the CalB activity measured in the respective microemulsions. The enzyme activity was measured at each temperature with 0.5, 1, 2 and 3 mg mL<sup>-1</sup> of CalB.

nitrophenol formed for each substrate throughout the reaction.

The reactions were monitored until completion to detect any inhibitory effects that could be caused by the substrates or products. The yield obtained after 10 h indicates a clear dependency on the chain length of the substrate, with 75% for *p*-nitrophenyl caprylate, 80% for *p*-nitrophenyl laurate and 90% for *p*-nitrophenyl palmitate. However, the observed second order rate constants  $k_2$  were found to be similar, namely  $0.14 \times 10^{-3} \text{ L s}^{-1} \text{ g}^{-1}$  for *p*-nitrophenyl caprylate,  $0.17 \times 10^{-3} \text{ L s}^{-1} \text{ g}^{-1}$  for *p*-nitrophenyl laurate and  $0.13 \times 10^{-3} \text{ L s}^{-1} \text{ g}^{-1}$  for *p*-nitrophenyl palmitate. To study the CalB activity with increasing substrate concentrations, *p*-nitrophenyl laurate had to be used instead of *p*-nitrophenyl palmitate due to solubilisation problems of the latter in *n*-octane. The microemulsions used were of the same composition as before with the only difference that the amount of substrate in the oil phase was varied. The resulting phase diagrams can be seen in Figure 5 (top). As can be seen, the phase inversion temperature decreases with increasing substrate concentration, which is why the reaction temperatures were slightly different, or, more precisely, between 44 and 41 °C. Figure 5 (bottom) shows the obtained initial reaction rates for the hydrolysis of *p*-nitrophenyl

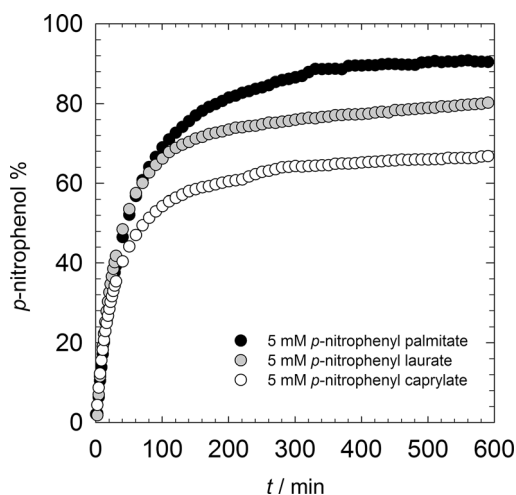


**Figure 4.** The CalB-catalysed hydrolysis of *p*-nitrophenyl palmitate, -laurate and -caprylate in a bicontinuous microemulsion liberates *p*-nitrophenol. The amount of formed *p*-nitrophenol is calculated from the absorbance at the isosbestic wavelength and is plotted as a function of time. The microemulsions consisted of buffer pH 7-*n*-octane/5 mM substrate- $C_{10}E_5$ . The enzyme concentration was  $3 \text{ mg mL}^{-1}$  in the aqueous phase and the microemulsion was prepared at  $\phi=0.5$ ,  $\gamma=0.175$  and  $T=44^\circ\text{C}$ .

laurate in a concentration range of 5–60 mM. The CalB activity was found to be a linear function of the substrate concentration. To find out whether the small temperature differences influence the initial reaction rate, three substrate concentrations were measured at two temperatures: 20 mM at 44 and  $43^\circ\text{C}$ , 40 mM at 43 and  $42^\circ\text{C}$  and 60 mM at 42 and  $41^\circ\text{C}$ . The obtained initial reaction rates are also plotted in Figure 5 (bottom) and it is obvious that temperature differences of  $\pm 1^\circ\text{C}$  have only a very small effect on the CalB activity.

#### Influence of the concentration of CalB on its activity

Previous kinetic studies of lipase-catalysed reactions performed in *w/o*-microemulsions reported the presence of lag times,<sup>[19]</sup> which are explained by the use of the injection method (i.e., injecting an enzyme solution into an already formed microemulsion). Delays or lag times are observed when the adsorption of the enzyme is slower than the reaction kinetics.<sup>[20]</sup> As we also used the injection method, we studied first possible delays in the reaction kinetics. For this purpose, the adsorption of CalB at a buffer/*n*-octane interface was followed by interfacial tension measurements and then compared with reaction kinetics measured at different CalB concentrations, focussing on very small CalB concentrations. Figure 6 (top) shows the interfacial tension measurements between *n*-octane and buffer solutions containing 0.025, 0.075, 0.25, 0.4, 0.5, 1 and  $3 \text{ mg mL}^{-1}$  CalB, which were carried out at room temperature. In Figure 6 (bottom) the corresponding CalB activities in the microemulsions are presented. The curves seen in Figure 6 (top) are typical for interfacial tension measurements with proteins.<sup>[21]</sup> At low CalB concentrations, the induction time can be observed, that is the time it takes for CalB to adsorb without significantly reducing the interfacial tension  $\gamma_{ab}$ . Once a suffi-

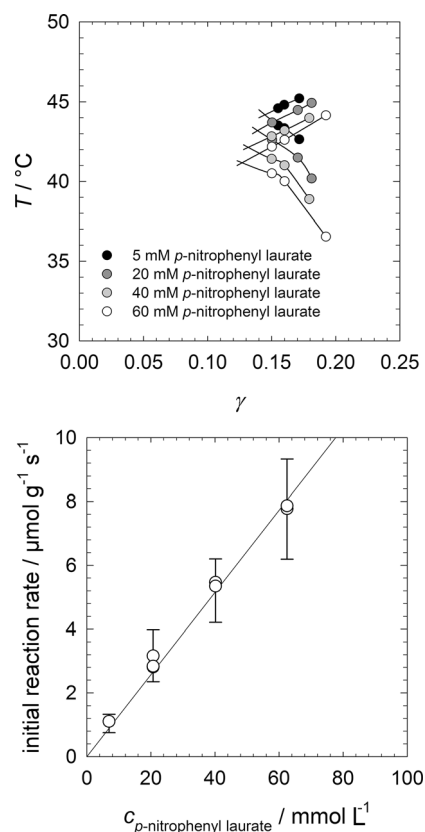


**Figure 5.** Top: phase diagrams of microemulsions consisting of buffer pH 7-*n*-octane/*p*-nitrophenyl laurate- $C_{10}E_5$  with increasing *p*-nitrophenyl laurate concentrations from 5–60 mM. Bottom: initial reaction rates of the CalB-catalysed hydrolysis of *p*-nitrophenyl laurate in the microemulsion as a function of the substrate concentration. The microemulsions were prepared at  $\phi=0.5$  and  $\gamma=0.175$  and at temperatures between  $T=44$  and  $41^\circ\text{C}$  according to the location of the X-point at the respective *p*-nitrophenyl laurate concentration. Please note that the initial reaction rate is normalised by the CalB concentration, which is given in  $\text{mg mL}^{-1}$ .

cient amount of CalB is adsorbed, the interfacial tension  $\gamma_{ab}$  drops sharply, until an equilibrium interfacial tension is reached. At high CalB concentrations, the induction time and sometimes even the time period in which  $\gamma_{ab}$  drops down to the equilibrium value is out of the detectable time range. At the highest CalB concentration of  $3 \text{ mg mL}^{-1}$  only the equilibrium interfacial tension value could be detected.

After having observed that even small concentrations of CalB adsorb relatively fast at the buffer/*n*-octane interface, the CalB activity in the microemulsion was measured. By way of an example, for  $0.25 \text{ mg mL}^{-1}$  of CalB the equilibrium value is reached after 100 s. As interfacial tension measurements and adsorption times are sensitive to temperature, we could not use our model system since the phase inversion temperature of the model system is  $\tilde{T}=44^\circ\text{C}$ , whereas the interfacial tension study was carried out at room temperature. Thus the microemulsion consisting of buffer-*n*-octane/5 mM *p*-nitrophenyl palmitate- $C_{10}E_4$  ( $\gamma_{\text{Reaction}}=0.141$ ) was used for the kinetic measurements since it has a phase inversion temperature close to room temperature ( $\tilde{T}=23^\circ\text{C}$ ) so that interfacial tension and initial reaction rates can be compared directly. Figure 6 (bottom)

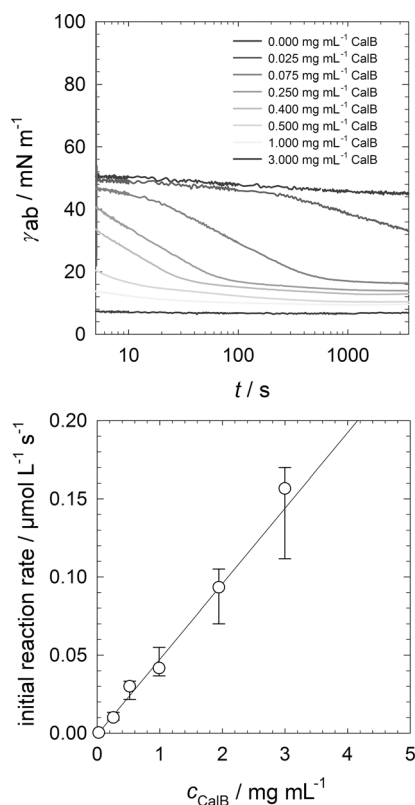


**Figure 6.** Top: interfacial tension  $\gamma_{ab}$  between buffer (pH 7) and *n*-octane as a function of time. The samples contained either no or up to  $3 \text{ mg mL}^{-1}$  CalB in the aqueous phase. Bottom: initial reaction rates of the CalB-catalysed hydrolysis of *p*-nitrophenyl palmitate in a microemulsion consisting of buffer pH 7–*n*-octane/5 mM *p*-nitrophenyl palmitate– $\text{C}_{10}\text{E}_4$  at  $23^\circ\text{C}$  as a function of the initial CalB concentration  $c_{\text{CalB}}$ . The microemulsion was prepared at  $\gamma = 0.141$  and  $\phi = 0.5$ .

shows the initial reaction rates plotted against the CalB concentration. Since no lag time was observed during the measurements, we conclude that the reaction immediately started at all studied CalB concentrations (resolution limit was a lag time of less than one minute). As can be seen in Figure 6, the CalB activity was found to be a linear function of the CalB concentration. The adsorption of the CalB at the interfacial layer of the microemulsion and the rearrangement of the microemulsion system after the perturbation of adding the CalB solution was therefore fast enough to not cause any lag time in the detectable time range.

### Co-surfactants

The addition of co-surfactants to the system can help to understand how the composition of the interfacial layer affects the CalB activity. Two different co-surfactants were chosen, namely the hydrophobic phospholipid 1,2-dioleoyl-*sn*-glycero-3-phosphocholine (DOPC) and the hydrophilic sugar surfactant *n*-decyl- $\beta$ -D-glucopyranoside ( $\beta$ - $\text{C}_{10}\text{G}_1$ ). Due to different properties, they could not be used at the same co-surfactant mass fraction  $\delta$ . Phospholipids on the one hand are strongly amphiphilic and form very efficient microemulsions, but also tend to stabilize liquid crystalline phases. To keep the formation of

liquid crystalline phases at a minimum, only a co-surfactant mass fraction of  $\delta$  (DOPC) = 0.05 could be used. Sugar surfactants, on the other hand, have a strongly hydrated head group at nearly all temperatures and the maximum possible co-surfactant mass fraction (without losing the temperature-sensitivity of the microemulsions), was  $\delta$  ( $\beta$ - $\text{C}_{10}\text{G}_1$ ) = 0.50. Due to very high phase inversion temperatures in the presence of the sugar surfactant, it was necessary to add 18 wt% NaCl to the aqueous phase of these microemulsions to decrease the phase inversion temperature so that the system can be compared with the other systems in the present study. As the CalB activity has been proven to be quite temperature-dependent, the influence of the co-surfactants was tested over the same temperature range as before the  $\text{C}_{10}\text{E}_j$  microemulsions. The microemulsions were prepared as explained previously by using different  $\text{C}_{10}\text{E}_j$  surfactants to obtain phase inversion temperatures in the range of  $20$ – $50^\circ\text{C}$ .

The resulting systems were buffer–*n*-octane/5 mM *p*-nitrophenyl palmitate– $\text{C}_{10}\text{E}_j$ /DOPC and buffer/18 wt% NaCl–*n*-octane/5 mM *p*-nitrophenyl palmitate– $\text{C}_{10}\text{E}_j$ / $\beta$ - $\text{C}_{10}\text{G}_1$ . Table 2 shows the *X*-points of each microemulsion, indicating the number of polyethylene glycol groups *j* of the  $\text{C}_{10}\text{E}_j$  surfactants for each system. The respective phase diagrams can be found in Figure S3 in the Supporting Information. Each of these systems was then used to measure the CalB activity towards the hydrolysis of *p*-nitrophenyl palmitate at the respective phase inversion temperature  $\tilde{T}$  and the surfactant mass fraction  $\gamma_{\text{Reaction}}$  determined from the phase diagrams.

**Table 2.** *X*-points of the systems consisting of buffer pH 7–*n*-octane/5 mM *p*-nitrophenyl palmitate– $\text{C}_{10}\text{E}_j$ /DOPC and buffer pH 7/18 wt% NaCl–*n*-octane/5 mM *p*-nitrophenyl palmitate– $\text{C}_{10}\text{E}_j$ / $\beta$ - $\text{C}_{10}\text{G}_1$ .<sup>[a]</sup>

<i>j</i>	$\text{C}_{10}\text{E}_j$ /DOPC		$\text{C}_{10}\text{E}_j$ / $\beta$ - $\text{C}_{10}\text{G}_1$	
	$\tilde{\gamma}$	$\tilde{T}$ [ $^\circ\text{C}$ ]	$\tilde{\gamma}$	$\tilde{T}$ [ $^\circ\text{C}$ ]
4	0.089	23	0.088	24
4.5	0.092	32	0.117	31
5	0.112	43	0.127	39
5.5	0.127	50	0.142	44
6	–	–	0.160	50

[a]For each system the number of ethylene glycol groups *j* is indicated.

Figure 7 shows the resulting CalB activities as observed second order rate constants  $k_2$  plotted against temperature. The system containing only  $\text{C}_{10}\text{E}_j$  surfactant without co-surfactants is plotted again for comparison. In the observed temperature range, CalB was active in all investigated systems. The highest CalB activity was found at temperatures of  $40$ – $45^\circ\text{C}$  regardless of the composition of the interfacial layer. The absolute values for the observed second order rate constants  $k_2$  vary with the composition of the interfacial layer. The co-surfactant DOPC was found to negatively influence the CalB activity, that is, lower CalB activities were observed compared to values obtained in the DOPC-free  $\text{C}_{10}\text{E}_j$  systems. On the other hand, the co-surfactant  $\beta$ - $\text{C}_{10}\text{G}_1$  enhanced the CalB activity, that is, higher CalB activities than those observed for the  $\text{C}_{10}\text{E}_j$  systems were found.

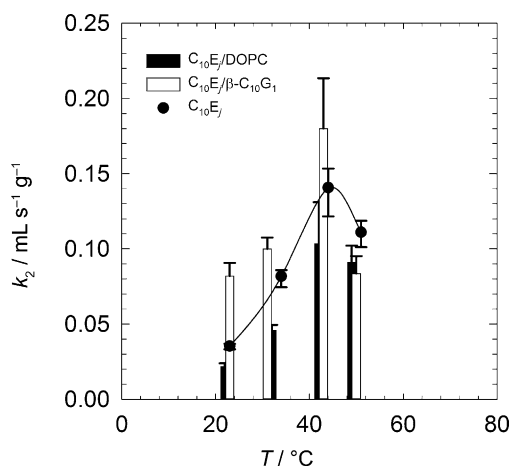


**Figure 7.** Influence of the temperature on the observed second order rate constants  $k_2$  of the CalB-catalysed hydrolysis of *p*-nitrophenyl palmitate. The microemulsions consisted of buffer pH 7-*n*-octane/5 mM *p*-nitrophenyl palmitate- $C_{10}E_j$ /DOPC ( $\delta = 0.05$ ) and buffer pH 7/18 wt% NaCl-*n*-octane/5 mM *p*-nitrophenyl palmitate- $C_{10}E_j/\beta$ - $C_{10}G_1$  ( $\delta = 0.50$ ). The different temperatures were realised by changing  $j$  in the  $C_{10}E_j$  surfactants. The microemulsions were prepared at  $\phi = 0.5$  and  $\gamma_{\text{Reaction}} = \bar{\gamma} + 0.02$ . The temperature dependence of the  $k_2$  values obtained for the microemulsion containing only  $C_{10}E_j$  surfactants is plotted for comparison.

## Discussion

CalB activity in bicontinuous microemulsions is affected by both NaCl content and temperature. The addition of NaCl decreases the enzymatic activity because it changes the ionic interactions. These changes could decrease the adsorbed amount of CalB molecules at the interfacial layer or affect the CalB conformation. The reduced amount of adsorbed lipase molecules at interfaces through increase of the NaCl content has been reported for different systems, such as a membrane reactor system<sup>[22]</sup> and an ionic liquids system.<sup>[23]</sup> To investigate if the NaCl content is influencing the activity of CalB in a two-phase system, we carried out a reaction in a two-phase system containing a stock solution of substrate in *n*-octane and 100 mM TRIS buffer pH 7 with either 0, 4 or 18 wt% NaCl. The results clearly showed a decrease of the obtained yields when analysed after 24 h, as shown in Figure S4 in the Supporting Information. Due to the fact that in the two-phase system the only possible contact between enzyme and substrate is at the macroscopic interface, desorption of CalB from this macroscopic interface could explain the observed trend. With regards to the influence of the NaCl content on the conformation of CalB, circular dichroism measurements in aqueous solutions showed no significant changes of the secondary conformation of CalB, even in the presence of 18 wt% NaCl (Figure S5 in the Supporting Information). Nevertheless, it is possible that the conformation of the CalB molecules that are adsorbed at the interfacial layer is more sensitive to unfavourable ionic interactions.

The correlation between temperature and CalB activity revealed a maximum CalB activity at 44 °C, which is higher than in conventional reaction media. For instance, in aqueous solution the maximum activity of a mixture of CalA and CalB is at 35 °C.<sup>[24]</sup> An enhancement of the thermostability of lipases was

previously reported for lecithin reverse micelles and was explained with a different water activity.<sup>[25]</sup>

Studying the influence of temperature and ionic strength on the activity of CalB in bicontinuous microemulsions was only possible by changing the hydrophilicity of the surfactant. This, unfortunately, also affects the domain sizes of the microemulsion because different surfactants have different efficiencies. However, by looking at the *X*-points listed in Table 1, we see that the efficiency does not change significantly, which, in turn, means that the domain size stays more or less the same. Nevertheless, a systematic study on the influence of the domain size of the bicontinuous microemulsion on the enzymatic activity would be the next logical step.

The dependence of the CalB activity on the alkyl chain length of the substrate revealed two interesting points. Firstly, all the substrates are dissolved in the oil phase of the microemulsion. Therefore, and in contrast to what happens in conventional reaction media, no solubility problems are observed. This is why the differences between the initial rates are small. The slightly higher CalB activity towards the *p*-nitrophenyl laurate can be explained by the fact that the active site of CalB fits exactly for 13 C atoms<sup>[26]</sup> and that therefore the binding of *p*-nitrophenyl laurate is the most favourable one. The second interesting point concerns the obtained yield after 10 h. The results show that the longer the alkyl chain of the substrate, the better is the obtained yield, which can be explained with the inhibition of CalB by short-chain fatty acids. Inhibition of CalB and other lipases by alcohols and fatty acids are well known from esterification reactions, also for octanoic acid and lauric acid, which are formed as products in this study.<sup>[27]</sup>

It is also very interesting to note that a linear relationship between the substrate concentration and the CalB activity was found. In the present study no saturation of the CalB activity and therefore no Michaelis-Menten kinetics were observed. This is probably due to a quite high  $K_M$  as found in w/o-microemulsions,<sup>[28]</sup> so that the studied substrate concentrations were much lower than  $K_M$  ( $[S] \ll K_M$ ). In the present study, we did not further increase the substrate concentration due to the large differences in the resulting *X*-points, which would have made a comparison of the data very difficult.

Studying the CalB adsorption at an oil/water interface we found that at most CalB concentrations the interfacial tension needs about 100 s to reach the equilibrium value. This relatively fast adsorption time (compared to other proteins) correlates well with the kinetics measured at different CalB concentrations, in which no lag time was observed. The conclusion from these findings is that CalB adsorption at the oil/water interface is fast and that the reaction rate directly depends on the CalB concentration. The observed reaction rate therefore depends on both enzyme and substrate concentration, and no retarding effects are observed.

The composition of the interfacial layer influences the reaction rate of CalB-catalysed hydrolysis of *p*-nitrophenyl palmitate. Compared with the CalB activity observed in microemulsions formulated with  $C_{10}E_j$  alone, the addition of the co-surfactant DOPC led to lower CalB activities, while the addition of the sugar surfactant  $\beta$ - $C_{10}G_1$  enhanced the CalB activity. These

results can be explained by the hydrophilicity of the surfactant head group and its hydration level. The results showed that the CalB activity increases with the hydrophilicity of the surfactant. For instance, in the microemulsions prepared with sugar surfactant as co-surfactants, which is more hydrophilic than  $C_{10}E_5$  the activity of CalB was higher compared to the  $\beta$ - $C_{10}G_1$ -free system. These results are in agreement with studies performed in w/o-microemulsions, which identified hydrophilic surfactants with large head groups as promising surfactants for lipase-catalysed reactions.<sup>[11,15]</sup> The strong hydration of the sugar surfactant head group can also play an important role in providing water molecules especially at the interface and in stabilising the CalB even at high (18 wt%) NaCl contents. As a consequence, the strongly hydrated sugar surfactant head group might also prevent desorption of CalB from the interface, which was assumed to be the reason for the low CalB activity in microemulsions prepared with  $C_{10}E_j$  at high  $\varepsilon$ .

To better understand the systems, we determined the activation energies of reactions for the co-surfactant-free microemulsion as well as for the two microemulsions prepared with surfactant/co-surfactant mixtures. The apparent activation energy  $E_a$  was calculated according to the Arrhenius Equation and it was found to be  $32 \text{ kJ mol}^{-1}$  for the  $C_{10}E_5/\beta$ - $C_{10}G_1$  system,  $50 \text{ kJ mol}^{-1}$  for the co-surfactant-free  $C_{10}E_5$  system and  $60 \text{ kJ mol}^{-1}$  for the  $C_{10}E_5/\text{DOPC}$  system. The lowest apparent activation energy found for the microemulsion prepared with  $C_{10}E_5/\beta$ - $C_{10}G_1$  is comparable to the activation energies that were reported for lipase-catalysed reactions in droplet microemulsions.<sup>[25,29,30]</sup> The length of the alkyl chain of the substrate can also influence the activation energy. Indeed, the activation energy for hydrolysis of the esters seems to increase with increasing chain length of the ester, for example,  $20 \text{ kJ mol}^{-1}$  for *p*-nitrophenyl butyrate and  $44 \text{ kJ mol}^{-1}$  for *p*-nitrophenyl caprylate.<sup>[30]</sup> Additionally, one should note that the different  $\gamma_{\text{Reaction}}$  of the systems cannot cause the differences in activities since it holds  $\gamma_{\text{Reaction}}(C_{10}E_5/\text{DOPC}) < \gamma_{\text{Reaction}}(C_{10}E_5/\beta$ - $C_{10}G_1) < \gamma_{\text{Reaction}}(C_{10}E_5)$  whereas the activity follows  $k_2(C_{10}E_5/\text{DOPC}) < k_2(C_{10}E_5) < k_2(C_{10}E_5/\beta$ - $C_{10}G_1)$ .

## Conclusion

We have found a temperature dependence of the CalB activity in bicontinuous microemulsions that does not depend on the interfacial composition with a maximum activity around  $44^\circ\text{C}$ . The influence of NaCl was found to be more complex, with high NaCl contents found to be unfavourable for the CalB activity when the reactions were carried out in microemulsions prepared with  $C_{10}E_j$  surfactants, but not in the presence of sugar surfactant. Interfacial tension measurements between CalB solutions and *n*-octane revealed fast adsorption at nearly all concentrations, which supports our previous results that showed CalB preferably located at the interface. The linear dependence of the CalB activity on both enzyme and substrate concentrations showed that CalB-catalysed biotransformations are feasible in bicontinuous microemulsions and benefit from fast mass transport and enhanced enzyme–substrate contact at the interface.

## Experimental Section

### Enzyme and materials

All surfactants were purchased from Sigma (UK), namely tetraethylene glycol monodecyl ether ( $C_{10}E_4$ ) with a purity of  $\geq 97\%$ , pentaethylene glycol monodecyl ether ( $C_{10}E_5$ ) with a purity of  $\geq 97\%$ , hexaethylene glycol monodecyl ether ( $C_{10}E_6$ ) with a purity of  $\geq 99\%$ , octaethylene glycol monodecyl ether ( $C_{10}E_8$ ) with a purity of  $\geq 98\%$  and decyl  $\beta$ -D-glucopyranoside ( $\beta$ - $C_{10}G_1$ ) with a purity of  $\geq 98\%$ . The substrates *p*-nitrophenyl palmitate, *p*-nitrophenyl laurate and *p*-nitrophenyl caprylate and the products *p*-nitrophenol (in spectrophotometric grade) and palmitic acid ( $\geq 99\%$ ) were also purchased from Sigma, UK. The lipase B from *Candida antarctica* was purified and provided by the Institute of Technical Biochemistry, Stuttgart, Germany. The purification was performed by ion-exchange chromatography and the lyophilised purified protein was used to prepare the stock solutions.<sup>[31]</sup> For the preparation of the buffer solution, tris(hydroxymethyl)aminomethane with a purity of  $\geq 99.9\%$  was used. For the preparation of the microemulsions bi-distilled water, sodium chloride ( $\geq 99.5\%$ ) from Sigma, UK and *n*-octane ( $\geq 99\%$ ) purchased from Sigma, UK, was used.

### Preparation of the microemulsions

The parameters describing the composition of the microemulsion are described in the following Equations. The mass fraction of the surfactant in the total mixture is given by:

$$\gamma = \frac{m_{\text{Surfactant}}}{m_{\text{Surfactant}} + m_{\text{Oil}} + m_{\text{Buffer}}} \quad (1)$$

The mass fraction of the co-surfactant in the surfactant mixture is given by:

$$\delta = \frac{m_{\text{Co-surfactant}}}{m_{\text{Co-surfactant}} + m_{\text{Surfactant}}} \quad (2)$$

The oil-to-water ratio is either given by the mass fraction of the oil in the mixture of oil and aqueous phase

$$\alpha = \frac{m_{\text{Oil}}}{m_{\text{Oil}} + m_{\text{Buffer}}} \quad (3)$$

or by the corresponding volume fraction

$$\phi = \frac{V_{\text{Oil}}}{V_{\text{Oil}} + V_{\text{Buffer}}} \quad (4)$$

The mass fraction of NaCl in the total mass of the aqueous phase is:

$$\varepsilon = \frac{m_{\text{NaCl}}}{m_{\text{NaCl}} + m_{\text{Buffer}}} \quad (5)$$

The concentration of lipase in the water phase of the microemulsion is:

$$c_{\text{CalB}} = \frac{m_{\text{CalB}}}{V_{\text{Buffer}}} \quad (6)$$

For the preparation of bicontinuous microemulsions, equal volumes ( $\phi=0.5$ ) of a buffer solution with appropriate amounts of NaCl and *n*-octane were used. Where possible, stock solutions of substrate in *n*-octane were prepared, as well as stock solutions of lyophilised purified CalB in buffer. For the phase diagrams, 0.3 mL of oil phase and 0.3 mL of water phase was used, giving a total volume of 0.6 mL of oil and water. For the reactions, 0.075 mL of oil and 0.075 mL of water was used, giving a total volume of 0.15 mL of oil and water. The corresponding surfactant mass was calculated and the three components were weighed in with an accuracy of  $0.5 \times 10^{-3}$  g.

### Optical detection of phase behaviour

The microemulsions were prepared in a glass vial, which was closed with a plastic stopper and sealed with laboratory film. The vial was placed in a thermostated water bath equipped with a magnetic stirrer and a digital thermometer (accuracy 0.01 °C) next to the vial. The phase boundaries enclosing the one phase region at surfactant mass fractions  $\gamma > \hat{\gamma}$  were optically detected in an accuracy of  $\pm 0.5$  °C and extrapolated to the X-point. Anisotropic phases were detected by using crossed polarisers.

### Localisation of compounds in a three-phase microemulsion

To investigate the localisation of compounds in a microemulsion, a three-phase microemulsion was prepared at a surfactant mass fraction  $\gamma \ll \hat{\gamma}$  (in the present study  $\gamma = 0.08$ ). The microemulsion was equilibrated at the phase inversion temperature taken from the respective phase diagram. The samples were prepared in GC vials, sealed with laboratory film. After 24 h the individual phases were carefully removed through the septum, using a syringe with a needle. The spectra of the individual phases were measured in a Cary 100 spectrophotometer with a thermostated cell holder. Each of the phases were equilibrated and measured at the phase inversion temperature, to ensure that the microemulsion (i.e., the middle phase) was homogeneous and transparent.

### Measurement of reaction kinetics

According to the Michaelis–Menten kinetics, for  $K_M \gg [S]$ , the initial reaction rate  $v$  can be described as

$$v = \frac{k_{\text{cat}}[E][S]}{K_M} \quad (7)$$

and the second-order rate constant  $k_2 = k_{\text{cat}}/K_M$  can be introduced:

$$v = k_2[E][S] \quad (8)$$

Please note that the enzyme concentration  $[E] = c_{\text{CalB}}$  is given in  $\text{mg mL}^{-1}$  and thus the resulting unit for  $k_2$  is  $\text{L s}^{-1} \text{g}^{-1}$ . The initial reaction rate  $v$  is given by the slope of the linear increase of concentration versus time. For this purpose, the absorbance of the product *p*-nitrophenol was followed at the isosbestic wavelength for 20 min. To calculate the concentration of *p*-nitrophenol from the absorbance one needs to consider that the substrate also absorbs

at this wavelength to a small extent. The absorbance at a specific wavelength is described as

$$A = d \cdot \sum_i \epsilon_i \cdot c_i \quad (9)$$

in which  $A$  is the absorbance at a specific wavelength,  $d$  is the path length of the cuvette,  $\epsilon$  is the molar absorptivity and  $c$  is the concentration. The index  $i$  represents all components absorbing at this wavelength, in our case the substrate or the product *p*-nitrophenol. We can now write for the concentration of *p*-nitrophenol at a time  $x$  during the reaction

$$c_{p\text{NP},t=x} = \frac{\frac{A_{\lambda(\text{isob.})}}{d} - \epsilon_{\text{Substrate}} \cdot C_{\text{Substrate},t=0}}{(\epsilon_{p\text{NP}} - \epsilon_{\text{Substrate}})} \quad (10)$$

In the present work, all concentrations are initial concentrations in either the oil or the aqueous phase used to prepare the microemulsion.

To determine the isosbestic wavelength of the product, scans of *p*-nitrophenol in microemulsions containing buffer solutions at different pH values were taken. The molar absorptivity  $\epsilon$  measured according to the Beer–Lambert law was correlated with the initial concentration of *p*-nitrophenol in the aqueous phase and is therefore smaller than in aqueous solution due to the presence of oil and surfactant in the mixture. Hence, the molar absorptivity  $\epsilon$  was measured for each system.

The measurements were carried out using a Cary 100 spectrophotometer with a thermostated cell holder. For the measurement of the enzyme activity, the microemulsion was thermostated in the cell holder for 5 min before the reaction was started by adding the CalB solution. For this purpose, the microemulsion was initially prepared with 12.5  $\mu\text{L}$  less aqueous phase than oil phase, which was then added as a concentrated CalB solution to obtain the desired CalB concentration in the aqueous phase. Scans were taken from 600–200 nm, at least every 2 min. After the measurements, the sample was checked again to be in the one-phase region. An example of a kinetics measurement is shown in Figure S6 in the Supporting Information.

### Acknowledgements

We thank the EPSRC for funding. We also thank Dr. Sandra Engelskirchen, Dr. Bernd Nebel and Prof. Dr. Bernhard Hauer for fruitful discussions. The support of Dr. AnnMarie O'Donoghue to interpret the kinetic data is greatly acknowledged.

**Keywords:** biocatalysis · enzymes · esters · hydrolases · hydrolysis

- [1] P. Reis, K. Holmberg, H. Watzke, M. E. Leser, R. Miller, *Adv. Colloid Interface Sci.* **2009**, 147–148, 237–250.
- [2] R. Verger, *Trends Biotechnol.* **1997**, 15, 32–38.
- [3] R. Strey, *Colloid Polym. Sci.* **1994**, 272, 1005–1019.
- [4] E. M. Anderson, K. M. Larsson, O. Kirk, *Biocatal. Biotransform.* **1998**, 16, 181–204.
- [5] a) J. Uppenberg, M. T. Hansen, S. Patkar, T. A. Jones, *Structure* **1994**, 2, 293–308; b) J. Uppenberg, N. Oehrner, M. Norin, K. Hult, G. J. Kleywegt, S. Patkar, V. Waagen, T. Anthonsen, T. A. Jones, *Biochemistry* **1995**, 34,

- 16838–16851; c) C. Li, T. Tan, H. Zhang, W. Feng, *J. Biol. Chem.* **2010**, *285*, 28434–28441; d) M. Martinelle, M. Holmquist, K. Hult, *Biochim. Biophys. Acta Lipids Lipid Metab.* **1995**, *1258*, 272–276; e) V. Ferrario, C. Ebert, L. Knapic, D. Fattor, A. Basso, P. Spizzo, L. Gardossi, *Adv. Synth. Catal.* **2011**, *353*, 2466–2480.
- [6] A. Schmid, J. S. Dordick, B. Hauer, A. Kiener, M. Wubbolts, B. Witholt, *Nature* **2001**, *409*, 258–268.
- [7] a) V. Gotor-Fernández, R. Brieva, V. Gotor, *J. Mol. Catal. B* **2006**, *40*, 111–120; b) T. Tan, J. Lu, K. Nie, L. Deng, F. Wang, *Biotechnol. Adv.* **2010**, *28*, 628–634; c) M. M. Soumanou, M. Pérignon, P. Villeneuve, *Eur. J. Lipid Sci. Technol.* **2013**, *115*, 270–285; d) C. M. Clouthier, J. N. Pelletier, *Chem. Soc. Rev.* **2012**, *41*, 1585–1605; e) P. Adlercreutz, *Chem. Soc. Rev.* **2013**, *42*, 6406–6436; f) K. Jaeger, B. Dijkstra, M. Reetz, *Annu. Rev. Microbiol.* **1999**, *53*, 315–351.
- [8] M. Breuer, K. Ditrich, T. Habicher, B. Hauer, M. Keßler, R. Stürmer, T. Zelinski, *Angew. Chem. Int. Ed.* **2004**, *43*, 788–824; *Angew. Chem.* **2004**, *116*, 806–843.
- [9] R. Kourist, P. Dominguez de Maria, K. Miyamoto, *Green Chem.* **2011**, *13*, 2607–2618.
- [10] a) H. Stamatis, A. Xenakis, F. N. Kolisis, *Biotechnol. Adv.* **1999**, *17*, 293–318; b) K. Martinek, A. V. Levashev, N. Klyachko, Y. L. Khmel'nitski, I. V. Be-rezin, *Eur. J. Biochem.* **1986**, *155*, 453–468.
- [11] D. Das, S. Roy, R. N. Mitra, A. Dasgupta, P. K. Das, *Chem. Eur. J.* **2005**, *11*, 4881–4889.
- [12] a) M. Laupheimer, S. Engelskirchen, K. Tauber, W. Kroutil, C. Stuben-rauch, *Tenside Surfactants Deterg.* **2011**, *48*, 28–33; b) M. Sathishkumar, R. Jayabalan, S. Mun, S. Yun, *Bioresour. Technol.* **2010**, *101*, 7834–7840; c) S. Wellert, B. Tiersch, J. Koetz, A. Richardt, A. Lapp, O. Holderer, J. Gäb, M.-M. Blum, C. Schulreich, R. Stehle, *Eur. Biophys. J.* **2011**, *40*, 761–774.
- [13] N. Zhang, W. C. Suen, W. Windsor, L. Xiao, V. Madison, A. Zaks, *Protein Eng.* **2003**, *16*, 599–605.
- [14] U. K. Winkler, M. Stuckmann, *J. Bacteriol.* **1979**, *138*, 663–670.
- [15] D. Das, P. K. Das, *Langmuir* **2003**, *19*, 9114–9119.
- [16] M. Subinya, A. K. Steudle, B. Nestl, B. Nebel, B. Hauer, C. Stubenrauch, S. Engelskirchen, *Langmuir* **2014**, *30*, 2993–3000.
- [17] S. Burauer, T. Sachert, T. Sottmann, R. Strey, *Phys. Chem. Chem. Phys.* **1999**, *1*, 4299–4306.
- [18] A. L. Ong, A. H. Kamaruddin, S. Bhatia, W. S. Long, S. T. Lim, R. Kumari, *Enzyme Microb. Technol.* **2006**, *39*, 924–929.
- [19] M. B. Stark, P. Skagerlind, K. Holmberg, J. Carlfors, *Colloid Polym. Sci.* **1990**, *268*, 384–388.
- [20] S. Avramiotis, P. Lianos, A. Xenakis, *Biocatal. Biotransform.* **1996**, *14*, 299–316.
- [21] R. Miller, V. B. Fainerman, A. V. Makievski, J. Krägel, D. O. Grigoriev, V. N. Kazakov, O. V. Sinyachenko, *Adv. Colloid Interface Sci.* **2000**, *86*, 39–82.
- [22] W. Pronk, G. Boswinkel, K. van't Riet, *Enzyme Microb. Technol.* **1992**, *14*, 214–220.
- [23] Y. Jiang, C. Guo, H. Xia, I. Mahmood, C. Liu, H. Liu, *J. Mol. Catal. B* **2009**, *58*, 103–109.
- [24] M. Adamczak, *Pol. J. Food Nutr.* **2003**, *12*, 3–8.
- [25] J.-P. Chen, K.-C. Chang, *J. Ferment. Bioeng.* **1993**, *76*, 98–104.
- [26] J. Pleiss, M. Fischer, R. D. Schmid, *Chem. Phys. Lipids* **1998**, *93*, 67–80.
- [27] a) C. G. Lopresto, V. Calabrò, J. M. Woodley, P. Tufvesson, *J. Mol. Catal. B* **2014**, *110*, 64–71; b) G. D. Yadav, P. S. Lathi, *J. Mol. Catal. B* **2004**, *27*, 113–119; c) N. A. Serri, A. Kamaruddin, W. Long, *Bioprocess Biosyst. Eng.* **2006**, *29*, 253–260.
- [28] a) R. Schomaecker, B. H. Robinson, P. D. I. Fletcher, *J. Chem. Soc. Faraday Trans. 1* **1988**, *84*, 4203–4212; b) T. P. Valis, A. Xenakis, F. N. Kolisis, *Biocatal. Biotransform.* **1992**, *6*, 267–279.
- [29] D. Prazeres, F. Garcia, J. Cabral, *J. Chem. Technol. Biotechnol.* **1992**, *53*, 159–164.
- [30] G. E. Crooks, G. D. Rees, B. H. Robinson, M. Svensson, G. R. Stephenson, *Biotechnol. Bioeng.* **1995**, *48*, 190–196.
- [31] P. Trodler, J. Nieveler, M. Rusnak, R. D. Schmid, J. Pleiss, *J. Chromatogr. A* **2008**, *1179*, 161–167.

---

Received: September 18, 2014

Published online on December 15, 2014